LEGIBILITY NOTICE

A major purpose of the Technical Information Center is to provide the broadest dissemination possible of information contained in DOE's Research and Development Reports to business, industry, the academic community, and federal, state and local governments.

Although a small portion of this report is not reproducible, it is being made available to expedite the availability of information on the research discussed herein.

LA-UR

Received by OSTI

1989

TITLE COMPUTER SIMULATIONS OF EXPLOSIVE VOLCANIC ERUPTIONS

LA-UR--89-1928

DE89 014024

AUTHOR(S) Kenneth H. Wohletz and Greg A. Valentine

SUBMITTED TO Proceedings of the 28th International Geological Survey
Washington, DC
July 9-19, 1989

ABSTRACT

Today's large, high-speed computers provide capability for solution of the full set of two-phase, compressible Navier-Stokes equations in two or three dimensions. We have adapted computer codes that provide such solutions in order to study explosive volcanic phenomena. At present these fully nonlinear conservation equations are cast in two-dimensional cylindrical coordinates, which with closure equations comprise 16 equations with 16 unknown variables. Solutions for several hundred seconds of simulated eruption time require two to three hours of a Cray-1 computer time. Over 100 simulations have been run to simulate the physics of highly unsteady blasts, sustained and steady Plinian eruptions, fountaining column eruptions, and multiphase flow of magma in lithospheric conduits. The unsteady-flow calculations show resemblance to shock-tube physics with propagation of shock waves into the atmosphere and rarefaction waves down the volcanic conduit. Steady-flow eruption simulations demonstrate the importance of supersonic flow and overpressure of erupted jets of tephra and gases in determining whether the jet will buoyantly rise or collapse back to the earth as a fountain. Flow conditions within conduits rising through the lithosphere determine eruptive conditions of overpressure, velocity, bulk density, and vent size. Such conditions within conduit systems are thought to be linked to low frequency, sustained seismicity known as volcanic tremor. These calculations demonstrate the validity of some analytical eruption calculations under limited conditions. In general, though, the simulations show that consideration of nonlinearities inherent in multiphase properties, compressibility, and multiple dimensions lead to solutions that may greatly vary from simple, one dimensional analytical approaches and often produce results not available to intuitive reasoning.

INTRODUCTION

Computers have played an increasing role in geosciences over the last several decades in a variety of capacities, including data bases, digital mapping, geophysical data inversion, statistical analysis, and modeling or simulation of physical and chemical processes, to name a few. We discuss one of the newer applications, simulation based upon solution of sets of differential equations that model the fundamental physical relationships of fluid mechanics. Historically computers, especially those now called "supercomputers," were developed because of the vision of John Von Neumann (Ulam, 1980; Von Neumann and Richtmeyer, 1949), who believed that all the necessary fundamental physical relationships of fluid mechanics could be accurately expressed by mathematical relationships. Von Neumann realized that the intrinsic nonlinearity of these systems of differential equations and the large number of variables involved precluded analytical solution. He showed that mathematical techniques of finite differences could provide very precise solutions to individual equations, but that to perform such calculations would be practically impossible without utilization of machines that could rapidly process the billions of arithmetic steps required. Today we have those fast, large-memory machines, and continued evolution of the machines promises to soon achieve Von Neumann's vision.

Explosive volcanism plays an important role in todays understanding of geodynamic relationships. It represents the high flux endmember of mass and energy transport through the earth's lithosphere and is a major contributor to the chemical budget of the atmosphere. There is a growing understanding of the relationship of explosive volcanism to the chemical and physical character of the lithosphere and features of mantle dynamics. All of these interact in a strongly coupled system.

Our present capability of computer simulations of explosive volcanic eruptions has developed over the last decade through the stimuli of research

programs at Los Alamos focussed at understanding geothermal systems developed in calderas, modest efforts of characterizing and predicting volcanic hazards, and a large effort to bring the power of computational physics into the realm of earth sciences. This latter effort has followed a general, whole-earth approach in which large-scale behavior and character of the earth's core and mantle, plate and atmospheric dynamics, and fluid migration within the lithosphere are viewed as a coupled system. It is our hope that by gaining a confident ability to simulate the visible aspects of explosive eruptions, we can constrain some part of the lithospheric system through which magma migration occurs.

The following description of our explosive volcanism simulations will briefly review some geologic phenomena we attempt to model, the modeling approach we have adapted from other fields of computational physics, and results of simulations for endmember types of explosive behavior, including unsteady or "blast" eruptions, steady flows producing high standing tephra columns, eruptive "fountains", and finally our ongoing research into the character of flow in subsurface conduits.

Explosive Volcanic Phenomena

Explosive eruptive phenomena are highly variable, because of the large number of thermodynamic, chemical, and physical behaviors of magma and solid rocks through which it erupts. These phenomena have been classified by volcanologists by overall features of the eruptions and according to which type locality volcano the eruptions resemble (MacDonald, 1972; Walker, 1973). From physical points of view, the classification can be further simplified by consideration of the general fluid dynamical flow regime within which various eruptions are thought to behave (e.g. Wilson, 1980).

Caldera evolution sequence. Silicic calderas are generally thought to form in volcanoes that have demonstrated highly explosive or very large mass-flux eruptions. During their long histories of development, commonly over several million years with evolution of upper crustal magma chambers, having volumes of up to several thousands of cubic kilometers, eruptive behaviors range from passive lava extrusions to short-lived explosive blasts to prolonged jetting of large volumes of tephra and gases. Gradual chemical differentiation of such crustal magma chambers produces a volatile-rich chamber roof (Hildreth, 1979). During catastrophic release of overpressured volatiles from the top portion of the chamber, Smith (1979) estimates in general a 10 volume-percent drawdown of the magma reservoir, a volume which may be up to several hundreds of cubic kilometers. Wohletz et al. (1984) simulated such an eruption and showed that propagation of a rarefaction wave from the vent down into the chamber pressurized to 100 MPa stimulates vesiculation and fragmentation of the magma such that it erupts as an overpressured jet of hot pumice, ash, and gases. Initially the flow from the vent is unsteady, producing blast conditions of propagating shock waves in the atmospheric flow field. Gradually the flow becomes steady with generation of a high standing eruption column that may collapse in a fountain-like manner. After the magma chamber becomes largely depressurized, buoyant rise of viscous magma through the vent system produces lava domes and flows.

Plinian eruption columns and their collapse. Descriptions of the A.D. 79 explosive eruptions of Vesuvius, published by Plini the Younger, have led to specific definition of Plinian phenomena by Walker (1981), which includes high standing (10 - 50 km) eruption columns that sustain volume fluxes in excess of 10^6 m^3/s. These eruption columns are multiphase mixtures of pumice, ash, and gases (mostly steam) that show jet-like features at their bases and rise of a buoyant plumes near their tops (Sparks et al., 1978; Wilson et al., 1980). The flow is generally steady and displays considerable turbulence, which is thought to encourage mixing of the cooler atmosphere into the column. Heating of

admixed atmosphere by hot tephra can be sufficient to cause the column to rise buoyantly. If the atmospheric mixing is insufficient, such that the column remains denser than the atmosphere, the column may collapse in a fountain-like manner, spilling erupted debris and gases to the ground around the vent to produce ground-hugging flows called "pyroclastic flows."

Vulcanian and blast-type eruptions. Named after classical eruptive behavior of Vulcano in the Tyrrhenian Sea near Italy (Mercali and Silvestri, 1891), Vulcanian eruptions are generally described as repeated, cannon-like or staccato bursts of tephra with relatively small volume fluxes ($<< 10^6$ m^3/s) that form both hemispherically expanding clouds of tephra and gases and buoyantly rising plumes of several km height or less. The highly unsteady flow regime of these eruptions is can be accompanied by propagation of atmospheric shocks, temporal development of supersonic, overpressured jets, and development of laterally moving density currents of erupted ash called "pyroclastic surges." The unsteady and overpressured nature of such eruptions have characteristics similar to phenomena initiating larger Plinian events.

Strombolian and fountaining eruptions. Stromboli, the "light-house of the Mediterranean" is a volcano that displays short to prolonged bursts of tephra in ballistic trajectories from the vent. The expelled tephra in contrast to eruptions described above generally are not supported by an envelope of erupted gases. Rapid expansion of centimeter to meter sized gas bubbles propels tephra through the atmosphere. Where such activity is prolonged, a ballistic fountain is observed. Because such behavior results in rapid segregation of tephra from expanding gases, the expansion is nearly adiabatic in contrast to the Plinian and Vulcanian types in which gases remain in contact with the hot tephra and can expand nearly isothermally.

MODELING APPROACH

The mathematical formulation that we have used has been applied to wide variety of dispersed, multiphase flows, and it is discussed at length in the book by Ishii (1975). At the heart of the formulation is the assumption that the different materials involved in the flow field can be treated as individual continua; these continua are superimposed on each other and are coupled together by interphase transfer of mass, momentum, and energy. Because the different materials are treated as individual continua, the full set of conservation equations must be solved for each material (or field). The interphase transfer of transport quantities (mass, momentum, and energy) also requires that all equations for all fields must be solved simultaneously. It is clear that comprehensiveness of a model rapidly approaches the limits of modern computational speed and memory. For example, to model a two-dimensional, time-dependent, high-speed flow of gas and particles of three sizes would require the solution of 16 nonlinear partial differential equations (a set of four equations for the gas and for each particle size) and 20 additional algebraic equations (equations of state and interphase coupling) with 36 dependent variables. This example does not include mass transfer terms and would only be capable of including turbulence effects in the form of an eddy viscosity; solving more realistic turbulence transport equations such as those presented by Besnard and Harlow (1988) would at a minimum double the number of dependent variables.

As an aside, one might ask the question of why bother with numerical modeling if the models are so simplified in comparison to natural phenomena? The example described above shows how complex a numerical solution can be with only three particle sizes, one gas, and no mass transfer, and we know that volcanoes contain tephra particles ranging in size over several orders of magnitude with variable densities and shapes. Also, there are more than one gas species and mass transfer, involving exsolution of volatiles from tephra and their subsequent phase change. The answer to the above question is as

follows: although we can only model very crude approximations of nature, the approximations we do obtain provide behavioral insight that could not be obtained by intuition alone. The reason for this "beyond intuition" probe of natural processes derives from the intrinsic nonlinearity of the governing equations; many nonlinear processes are too complicated for mental solution even at an intuitive level; hence, the necessity of a sophisticated computing machine. Overall, we believe that gaining an understanding of relatively simple analogs to nature is prerequisite to grasping the complexities of nature. This reasoning is also the justification for laboratory experimentation; however, numerical simulation overcomes the problems of dynamic similarity that plague laboratory analogs.

Mathematical Formulation

Our modeling effort has focused on solving the following set of equations, forms of the complete Navier-Stokes equations, which describe a two-phase flow of compressible gas and incompressible solid particles:

$$\frac{\partial(\theta_g \rho_g)}{\partial t} + \nabla\cdot(\theta_g \rho_g \vec{u_g}) = J \tag{1}$$

$$\frac{\partial(\theta_s \rho_s)}{\partial t} + \nabla\cdot(\theta_g \rho_s \vec{u_s}) = -J \tag{2}$$

$$\frac{\partial(\theta_g \rho_g u_g')}{\partial t} + \nabla\cdot(\theta_g \rho_g \vec{u}\vec{u_g}) = -\theta_g \nabla p + K_g |\Delta u'| + J u_g' + \theta_g \rho_g g' \quad \nabla\cdot\tau_g \tag{3}$$

$$\frac{\partial(\theta_s \rho_s u_s')}{\partial t} + \nabla\cdot(\theta_s \rho_s \vec{u_s} u_s') = -\theta_s \nabla p + K_s |\Delta u'| - J u_s' + \theta_s \rho_s g' \quad \nabla\cdot\tau_s \tag{4}$$

$$\frac{\partial(\theta_g \rho_g I_g)}{\partial t} + \nabla\cdot(\theta_g \rho_g I_g \vec{u_g}) = -p\nabla\cdot[\theta_g \vec{u_g} + \theta_s \vec{u_s}] + R_g + |K_g|(\Delta \vec{u_g})^2 + J_e - \tau_g : \nabla \vec{u_g} \quad (5)$$

$$\frac{\partial(\theta_s \rho_s I_s)}{\partial t} + \nabla\cdot(\theta_s \rho_s \vec{u_s}) = R_s - J_e - \tau_s : \nabla \vec{u_s} \quad . \quad (6)$$

This formulation for two-phase flow (symbols defined in Table 1), presented by Harlow and Amsden (1975), is very general and has been successfully applied to a wide variety of flows from bubbly flow past an obstacle to star formation processes (Hunter et al., 1986). An important aspect of equations (1) through (6) is that they are cast in terms of volume-averaged quantities. The elemental volumes over which the differential equations are solved are necessarily much larger than the size of individual solid particles carried by the flow in order for the continuum approach to be valid (Travis et al., 1975).

Equations (1) and (2) are conservation of mass for the gas and solid phases, respectively. The left-hand side of these equations represents the sum of temporal and spatial changes of mass contained within an elemental volume. The right-hand sides are just the contribution to the gas phase by mass diffusion out of the solid.

Equations (3) and (4) express momenta conservation for the gas and solid phases, respectively. They state that the transient momentum changes within and advected through a volume element are balanced by the sum of forces due to the pressure gradient, interphase momentum transfer (drag), gravitational acceleration, momentum exchanged by interphase mass transfer, and viscous and turbulent stresses. Because explosive volcanic eruption columns have high Reynolds numbers, turbulent forces greatly dominate viscous ones, such that the last balancing term can be represented by the divergence of the strain-rate tensor using an eddy viscosity. The two-dimensional stress tensor has the following form, which crudely represents the Reynolds stress tensor:

$$\tau = -\theta \rho \nu_e \begin{bmatrix} 2\frac{\partial u}{\partial r} & 0 & \left[\frac{\partial v}{\partial r} + \frac{\partial u}{\partial z}\right] \\ 0 & 2\frac{u}{r} & 0 \\ \left[\frac{\partial v}{\partial r} + \frac{\partial u}{\partial z}\right] & 0 & 2\frac{\partial v}{\partial z} \end{bmatrix} \quad (7)$$

The eddy viscosity, ν_e, is constrained by observed eddy length scales and plays an important role in determining the mixing of atmosphere into the eruption column (Valentine and Wohletz, 1989). Although this description of turbulence is very crude and a more detailed calculation is being sought (e.g. Besnard and Harlow, 1988), we note that empirically derived turbulence representations have direct relationship with measurable physical features of flow, and theoretically derived ones are only poorly coupled with observation. For two-dimensional solutions, the momentum equations must be written for both components of velocity of the gas and solid phases.

Equations (5) and (6) are conservation of specific internal energy within a volume element for the gas and solid phases, respectively. The temporal and advected energy changes are equated to energy of pressure-volume work, interphase heat transfer, heat exchanged by phase changes, and energy dissipation by viscous stresses and turbulence. The gas phase also experiences changes in internal energy caused by interphase drag-induced dissipation.

These equations when written in expanded form comprise a system of eight, nonlinear, partial differential equations. Closure of the equations is obtained by applying algebraic relations that describe the equations of state for the materials, the relationship between volume fractions, and interphase coupling (see Valentine and Wohletz, 1989 for a detailed presentation of these terms). These algebraic closure equations account for the volume-averaged effects of processes that happen on a smaller scale than the elemental volume used for differentiation; for example, the drag of fluid on individual

particles. The very nature of this mathematical formulation requires that the microphysics are treated in only a very general sense. Thus many small-scale physical processes that are undoubtedly of importance in some volcanic phenomena are not included. Examples of such microphysics include particle-particle collisions, the particle-wake interactions, and distributions of bubble sizes in exsolving magmas. In principle the volume-averaged effects of any such process are implicitly included in the governing equations. For detailed simulation of a dense pyroclastic flow, we can introduce a pressure term to the equations for the particle phase that accounts for the normal stress produced by shearing grain flows. To date our simulations have focused on large-scale processes where most of the microphysical processes are thought to have negligible contribution.

A source of confusion in our simulations of eruption columns has been the role of turbulence in the governing equations, and how atmospheric entrainment is calculated. Previous eruption column models have been limited to one-dimensional, single-phase fluid approximations (see Woods, 1988 for a recent review and improvement of previous model attempts). In these approximations, a source term is required on the right-hand side of the conservation of mass equation in order to account for relatively cool atmosphere added to the flow by entrainment (i.e. the entrained fluid is added to the one-dimensional system). In our calculations, the atmosphere is part of the computational domain, and its entrainment naturally occurs as a result of turbulence diffusion in the momentum equation. In other words, the turbulent stress term in equations (3) and (4) produces a "force" that causes fluid movement in the same manner as any of the other terms in the momentum balance. Thus where a velocity gradient is present adjacent parts of the flow field will diffuse or interpenetrate into each other; the amount of interpenetration is proportional to the velocity gradient. Thus the gross effects of entrainment are included in the calculations. The details of this entrainment, which involve Kelvin-Helmholtz instability, are not strictly calculated but are solved in an averaged sense.

Although equations (1) through (6) are fairly comprehensive in that they include no restricting assumptions that might affect dynamic similarity, caution is required in applying their solutions to nature in the sense that they do not calculate "real" volcanoes. Because of the turbulence simplification and microphysical assumptions discussed above, the calculations are only valid in showing general eruption behaviors and relative variations that result from changes in initial and boundary conditions. We do not believe that it is realistic to directly apply numbers calculated by our models to natural systems, although that is a goal that Von Neumann believed is obtainable. Nevertheless, we can learn about the relative sensitivity of physical parameters involved, which is valuable for interpretation of field observations.

Computer Adaptation

Although mathematical solution techniques are available for attempting to get analytical solutions to the above equation set, it may be exceedingly difficult or impossible to get meaningful results after the required simplifications are made. Hence we have applied a numerical solution technique by finite differences (Ferziger, 1981). We begin by expanding the equations above into partial derivative form, using cylindrical coordinates (r,z,θ) with azimuthal symmetry along the z-axis, centered at the vent. The difference scheme used to discretize the partial derivatives on a constant spatially and temporally incremented grid was chosen to balance accuracy and stability with economy and versatility (Harlow and Amsden, 1975).

Finite difference solution scheme. A mixed, implicit explicit solution method, developed by Harlow and Amsden (1975), was chosen because of its economy and inherent numerical instabilities are easily rectified, even though a purely implicit differencing method of temporal derivatives is

generally more stable but more expensive. For example, the first term on the left-hand side of the continuity equation is written:

$$\frac{\partial \rho}{\partial t} \simeq \frac{\rho^{n+1} - \rho^{n}}{\delta t} \quad , \tag{7}$$

where the approximation signifies that of the finite differencing, and the index n represents the time step, such that there are $n = t/\delta t$ time steps of duration δt in a time period t. This forward differencing scheme explicitly gives the new value of ρ, ρu, ρv, or ρI with a truncation error of the order δt. Velocities are placed at cell edges for differencing advective terms to best model fluxes through cell edges. In order to circumvent stability problems in using cell-edge values of vectors, a staggered grid is defined and the advective term in the continuity equation is:

$$\frac{\partial \rho v}{\partial z} \simeq \frac{1}{\delta z} \left[\rho_{i,j} v_{i,j+1/2} - \rho_{i,j-1} v_{j-1/2} \right] \quad , \tag{8}$$

which holds for flow in the positive z direction. Such a scheme is called "donor cell" or "upwind" differencing, which ensures that the value advected into the a specific cell originates upstream. This scheme suppresses numerical instability, but steep gradients tend to be smeared over several cells, and the truncation error is kept to first order. For this reason, shocks in supersonic flows are not uniquely defined, but their presence can easily be distinguished in the solutions. Other nontrivial finite differences are those for stress tensors, which are solved for cell-edge values in the momentum equation and cell center quantities in the energy equation (Horn, 1986). For momentum and heat exchange terms in the conservation equations, an implicit form was chosen, because it is simple and unconditionally stable. In general the calculational time step proceeds by obtaining advanced time values for all scalar variables in the mesh, followed by a second iteration, during which new velocities are calculated, using new densities.

Because the systematics for solving the equation sets described above have been previously developed at Los Alamos for generalized application to hydrodynamics (e.g. Harlow and Amsden, 1975), it has been convenient to borrow sections of FORTRAN programs from other codes, making adaptations necessary for simulation of geological processes. In all cases, stability has been verified for the difference techniques (Hirt, 1968), such that we have high confidence for their applications over a large range of flow velocities.

Numerical output, graphical representation, and analytical approach. In general numerical results of each time step are dumped to disk storage for retrieval in the next time step, restarting the calculation, and generating tabular and graphical results. A typical calculation of 200 seconds of eruption time produces over 20,000 pages of tabulated numbers. A post-processor code can be applied to the dump files for various graphical outputs, including vector and contour plots and movies thereof. We have found that analysis of such voluminous results is time-consuming and difficult, such that a detailed study of an eruption simulation with initial and boundary conditions set to model a given volcano is analogous to a geological field study in which numerous field locations are examined to describe eruption effects and deposits.

It is instructive and useful to study simulation results for consistency with laboratory analogs and predictions, based upon other analytical solutions. As discussed below, the physics of high speed flows are known from laboratory experiments, and our computer results can be tested for their ability to reproduce known experiments. Once credibility has been established for a computer code, its results are considered to be "data" in that they are simply mathematical representations of physical parameters, as are say x ray analyses of rock chemical compositions, for which x ray intensities are converted by mathematical tools into numbers of chemical significance.

UNSTEADY DISCHARGE (BLAST-TYPE) ERUPTIONS

The concept of blast-type eruption was recently given a descriptive review by Kieffer (1982; 1984), and it includes eruptions that show highly unsteady, supersonic flow with notable propagations of shock waves, either as bow shocks that precede expulsions of tephra or as standing (Mach disk) shocks, that develop within supersonic jets of tephra and gases. Such eruptions are short-lived and in many places produce pyroclastic surge deposits of tephra. By analogy to large chemical or thermonuclear explosions, the presence of base surge deposits are often an earmark of highly unsteady flow and shock propagation (Glasstone and Dolan, 1977). As discussed above such eruptive phenomena are associated with initial phases of Plinian eruption and Vulcanian bursts.

Wohletz et al. (1984) modeled a large eruptive blast associated with Plinian eruptions that occur at during caldera-forming events. Assuming that an overpressured magma chamber can be nearly instantaneously opened to atmosphere by large scale vent rock failure, analogy to well known shock tube physics (Wright, 1967) is a convenient way to predict flow phenomena and to test the ability of our computer code to provide solutions that emulate those physics, which are described from consideration of mass and momentum conservation respectively written for one dimensional, inviscid flow:

$$\frac{\partial \rho}{\partial t} + \rho \frac{\partial u}{\partial x} + u \frac{\partial \rho}{\partial x} = 0 \qquad (9)$$

$$\frac{\partial u}{\partial t} + u \frac{\partial u}{\partial x} + \frac{1}{\rho} \frac{\partial p}{\partial x} = 0 \quad . \qquad (10)$$

Letting $f = \int c \, d\rho / \rho$, integrating from ρ_0 to ρ where $c = [\gamma(\partial p/\partial \rho)]^{1/2}$, and

substituting characteristic velocities, $dx/dt = u \pm c$, the conservation equations can be algebraically rewritten as:

$$\frac{\partial}{\partial t}(f + u) + (u + c)\frac{\partial}{\partial x}(f + u) = 0 \qquad (11)$$

$$\frac{\partial}{\partial t}(f - u) + (u - c)\frac{\partial}{\partial x}(f - u) = 0 \quad , \qquad (12)$$

Using and ideal equation of state where $p\rho^{-\gamma}$ equals a constant, the solution for f is, using the Riemann invariant for free expansion (Courant and Friedrichs, 1948):

$$f \qquad \frac{2c_0}{\gamma - 1}\left[\left(\frac{p}{p_1}\right)^{(\gamma-1)/2\gamma} - 1\right] \quad . \qquad (13)$$

Now with Rankine Hugoniot expressions for mass, momentum, and energy conservation across a shock wave (e.g. Shapiro, 1953), the flow field of a shock tube can be fully described by the following algebraic expressions:

$$\frac{u}{c_0} \qquad M\left(\frac{\gamma + \mu}{1 + \mu}\right) \qquad (14)$$

$$\frac{\rho}{\rho_0} \qquad \frac{(1 - \mu)(\gamma - 1)}{[(1 + \mu)(\gamma + \mu)]^{1/2}} \qquad (15)$$

$$\frac{\rho}{\rho_0} \qquad \frac{\mu + \gamma}{1 + \mu\gamma} \qquad (16)$$

$$\frac{T}{T_0} \qquad \frac{1 + \mu\gamma}{\mu + \gamma} \quad , \qquad (17)$$

for which the Mach number is $M = u/c_0$, the limit of isentropic expansion is $\mu = (\gamma - 1)/(\gamma + 1)$, and the y is the shock strength, p_1/p_2, which is a transcendental function of the atmospheric pressure p and chamber pressure p_0. The predictions of y and subsequent flow field variables are described in Wohletz et al. (1984) and are summarized in Figures 1 and 2.

We have found that our numerical codes nicely model shock-tube physics for two dimensions (Fig. 3). A blast-type eruption from a magma chamber at p_0 = 100 MPa, T_0 = 1273 K, and 8.7 wt % oversaturated with water from a vent with a hydraulic radius of about 100 m produces a bow shock of 3 MPa overpressure that exits the vent ahead of steam and tephra at about 1 km/s. Unsteady flow behind the shock continues up to several minutes as a rarefaction wave propagates down the conduit, accelerating the tephra to 300 to 500 m/s. Because the the rarefaction wave reflects off chamber walls, it causes surging flow out of the vent and development of a fluctuating Mach disk shock that adds to the blast phenomena. These results are shown in Figures 4 and 5.

STEADY DISCHARGE ERUPTIONS

Many explosive eruptions, especially those classified as Plinian, are thought to involve relatively long periods of approximately steady mass discharge once a vent has been opened (Walker, 1981). Depending on vent flow conditions, eruption columns may either rise as buoyant plumes from which tephra is deposited by fallout, or collapse in a fountaining manner from which tephra is emplaced by laterally flowing density currents (Sparks et al., 1978; Wilson et al., 1980; Valentine and Wohletz, 1989). Within the framework of our simulations, the conditions that determine whether an eruption column is buoyant or forms a fountain can be shown as a function of three dimensionless numbers (Fig. 6). These numbers are:

$$T_{gm} = \frac{p_e - p_{atm}}{(\rho_m - \rho_{atm})gR_v} = \frac{\text{pressure diving force}}{\text{buoyancy force}} \quad (18)$$

$$Ri_m = \frac{\rho_m v_e^2}{(\rho_m - \rho_{atm})gR_v} = \frac{\text{inertial force}}{\text{buoyancy force}} \quad (19)$$

$$K_p = \frac{p_e}{p_{atm}} = \frac{\text{exit pressure}}{\text{atmospheric pressure}} , \quad (20)$$

for which T_{gm}, the thermogravitational number, is a function of the exit (p_e) and atmospheric (p_{atm}) pressures, erupted column density (ρ_m) and atmospheric density (ρ_{atm}), gravitational acceleration (g), and vent radius (R_v); Ri_m, the Richardson number, includes the square of the exit velocity (v_e); and K_p is the pressure ratio. In order to arrive at the collapse criterion in Figure 6, we have considered eruptions with the same exit temperature (1200 K) and particle size (0.02 mm); a more comprehensive treatment would also include variation of these parameters. We note that our simulations of steady-flow eruptions have been limited to elevations of 7 km, and it is possible that that some columns that rise out of out domain might collapse from higher elevations. Still, the dimensionless numbers given above have strong physical significance in determining the behavior of erupted columns, and it is their relative influence that has been demonstrated by the numerical experiments.

Plinian eruption columns. The term "Plinian column," as discussed above, refers to eruptive phenomena of high-standing, buoyant plume of gas and tephra. Some results of an example simulation, producing and eruption column that exits the computational domain, are shown in Figure 7. As the flow initially exits the vent, it rapidly flares, owing to expansion from overpressure and the resistance of the atmosphere. The top of the column develops vorticity where it pushes against the atmosphere, and it is termed the "working surface," analogous to features seen in laboratory simulations of supersonic jets. As

time progresses, the working surface rises, and in the last snapshot, it is buoyantly rising out of the computational domain. In the two late-time snapshots a flaring structure typical of laboratory overpressured, supersonic jets (Kieffer and Sturtevant, 1984) is evident; it is a result of Prandtl-Meyer expansion of the jet as it exits the vent. Because the governing equations are the full Navier-Stokes equations with no restrictions on compressibility and other flow properties, the range of flow behaviors from subsonic to supersonic naturally occur in the calculations, and although as stated above, shock discontinuities (e.g. Mach disks) are numerically diffused over several cells, their effects are observable from plots of pressure and density contours and velocity vectors.

Eruption fountains and column collapse. When exit conditions of an eruption column plot below the surface shown in Figure 6, the column takes on a fountain like character (Fig. 8) that leads to formation of pyroclastic flows. In Figure 8 and example simulation is shown where most of the ash rises to about 3.5 to 4.0 km and then falls to the ground, forming both inward- and outward-moving pyroclastic flows. A low tephra-concentration cloud continuously rises off the pyroclastic flows. Figure 9 shows some of the properties of the pyroclastic flow at three different times during its evolution, the earliest of which corresponds to the time when the flow first hits the ground away from the vent. A parameter that is interesting from a geologic point of view is the dynamic pressure (Fig. 9b), which shows a complicated time evolution. For example, based upon effects of dynamic pressure, we predict that some locations away from the vent may experience a sequence of substrate erosion, followed by tephra deposition, while other locations experience the opposite sequence. Because the dynamic pressure can be directly related to bottom shear stress and hence erosion/deposition, we infer that even a simple eruption, such as we have numerically simulated, might lead to a very complex stratigraphy of tephra deposits. Eruptions with different exit conditions show widely varying dynamic pressure histories in their pyroclastic flows, indicating that the level of complexity that might be

interpreted from stratigraphic observations is essentially unlimited (Valentine and Wohletz, in press).

CONDUIT FLOW CALCULATIONS

The above simulations have used a wide variety of vent exit conditions. In reality, the exit velocities are strongly coupled to gas mass fraction, temperature, and pressure, as well as vent radius, all of which have been taken into consideration by Wilson et al. (1980) in a one-dimensional solution of flow within volcanic conduits. Because our solution technique is so very different than the analytical approach used by Wilson et al. (1980) (e.g. we consider two-dimensional solutions, including nonlinear and time-dependent processes), we feel that the actual range of exit parameters is still poorly constrained.

We are beginning calculations of flow through the lithosphere in conduits. This research, which was initially followed in the calculations of transient blast eruptions described above, requires more detailed work to fully constrain the range of possible exit parameters for steady eruption types. Included in our calculations are tracking of the rarefaction wave down the conduit, which is followed by a fragmentation surface where the gas phase becomes continuous, and the effects of volatile mass fraction and its phase change after exsolution from the magma. Also, we are calculating the effect of flow shear stress upon conduit walls that are deformable, erodible, and can add rock fragments to the flow. Figure 10 is a sketch of the flow field geometry we are solving.

A natural extension of flow calculations in lithospheric conduits is a study of source triggers for volcanic tremor, a collaborative study with

Bernard Chouet of the U. S. Geological Survey. Chouet (1986) describes the frequency content of volcanic tremors as seismic waves radiating from a fluid-filled crack in the lithosphere. Although the crack need not be connected to a volcanic conduit, there is certainly the possibility that such a crack represents part of a conduit system. The coupling of wave propagation in the fluid with elastic waves in the crack walls is nonlinear and results in a very slow wave called the "crack wave" by Chouet (1986). The source disturbance in the fluid is not known, but preliminary consideration of two-phase flow of a bubbly fluid and the growth and collapse of vapor bubbles in the fluid suggest that they are strong candidates for such a source trigger. This possibility is being investigated as a part of the conduit flow calculations.

SUMMARY

We have applied the separated, two-phase hydrodynamic equations, including all important physical parameters to modeling explosive volcanic eruptions. Two main types of eruption flow regimes are modeled: (1) unsteady, blast-type flow that involves highly transient effects, such as shock/rarefaction propagations and reflections and time-dependent flow within the volcanic conduit; (2) steady discharge eruptions in which vent exit conditions determine whether a high-standing, buoyant plume or a collapsing fountain are produced, the latter leading to development of pyroclastic flows. We have recently successfully reproduced some of the characteristics of the Mount St. Helens May 18, 1980 eruptions (Valentine and Wohletz, in press) and have early time calculations that support Kieffer's (1981) jet model for the blast phase of that eruption. Interestingly, we have found in those calculations that both a horizontal and a vertical jet orientation produces similar late time features.

The numerical simulations, being in essence experiments where the boundary and initial conditions are set by the operator with the results evolving

continuously through time, can provide much insight into various field observations, both of the activity of explosive eruptions and the tephra deposits that result. One example of this type of experimental observation is the pyroclastic flow erosion and depositional history mentioned above. Other examples include the flow dynamics that lead to depositional facies of pyroclastic flows, such as the ground surge that is commonly found at the base of pyroclastic flow deposits, the ash-cloud surge that is deposited over pyroclastic flow, and lateral depositional facies, determined by tephra size and volume concentration, such as proximal coignimbrite breccias. The simulations can aid in interpretation of active eruption behavior. For example, simulations show that the ash-cloud rising above a fountain can reach upward speeds much greater than the actual exit velocity at the vent, and that pyroclastic flow runout is affected by eruption-induced atmospheric convection (Valentine and Wohletz, 1989). Although numerical simulations can never completely substitute for observations of nature, they do have the advantage that one can see inside the flow, whereas in nature most of the important processes are hidden by veils of ash. Numerical simulations cannot stand alone, but they are in our opinion absolutely necessary for understanding most field observations of explosive volcanic activity.

An important lesson that we have learned from studying the multiphase hydrodynamics of explosive eruptions is that a rich complexity of processes is predicted by the relatively straightforward set of governing equations (eqs. 1-6). The diversity is a result of the inherent, nonlinear nature of these equations; small changes in parameters may produce very different solutions. This complexity suggests that for a given observation there may be several or more, equally plausible physical explanations, and that extreme caution should be used in interpretation of field observations, such as comparison of the phenomena of several different eruptions, even at the same volcano.

There are numerous directions that can be followed in future computer studies of explosive eruptions. One of these, the flow within volcanic

conduits through the lithosphere is our present track. Eventually, we will combine the conduit and external flow fields into one calculation, using a variable mesh size and time step. We have constrained our calculations to single particle sizes, and because the effect of multiple sizes is nonlinear, we have not attempted to superimpose solutions for simulations of different sizes. However, Marty Horn has developed a code at Los Alamos to calculate effects and trajectories of particles of various sizes and densities in a multiphase hydrodynamic calculation. Additional collaboration with Susan W. Kieffer of the U. S. Geological Survey will tackle a study of the detailed physics of the atmospheric flow field in a search for flow singularities and the effects of high particle concentrations, topographic barriers, and various column (jet) orientations.

ACKNOWLEDGEMENTS

We thank Eric Jones, Brook Sandford, Marty Horn, and Rod Whitaker for the years of support they have given in development and application of computer codes to geologic problems and especially their unique insight into physics of dynamic processes. Frank Harlow has been a great teacher of the methods of computational fluid dynamics, and he has encouraged and challenged us to build and improve on his work. Finally, Chick Keller, Sumner Barr, and Wes Myers have been instrumental in providing the administrative support for this work, which has been done under the auspices of the U. S. Department of Energy through the Office of Basic Energy Science and Institutional Supporting Research and Development at Los Alamos National Laboratory.

REFERENCES

Besnard D.C., and Harlow, F.H. (1988). 'Turbulence in multiphase flow', Int. J. Multiphase Flow, 14, 679-699.

Chouet, B. (1986). 'Dynamics of a fluid-driven crack in three dimensions by the finite difference method', J. Geophys. Res., 91, 13,967-13,992.

Courant, R., and Friedrichs, K.O. (1948). 'Supersonic flow and shock waves', in Pure and Applied Mathematics, Interscience, New York.

Ferziger, J.H. (1981). Numerical Methods for Engineering Applications, Wiley, New York

Glasstone, S., and Dolan, P.J. (1977). The Effects of Nuclear Weapons, U. S. Department of Defense and U. S. Department of Energy, Washington, D.C..

Harlow, F.H., and Amsden, A.A. (1975). 'Numerical calculation of multiphase fluid flow', J. Comput. Phys., 17, 19-52.

Hildreth, W. (1979). 'The Bishop Tuff: Evidence for the origin of compositional zonation in silicic magma chambers', Geol. Soc. Amer. Spec. Pap., 180, 43-75.

Hirt, C.W. (1968). 'Heuristic stability theory for finite-difference equations', J. Comput. Phys., 2, 339-355.

Horn, M. (1986). Physical Models of Pyroclastic Clouds and Fountains, M.S. Thesis, Arizona State University, Tempe.

Ishii, M. (1975). Thermo-Fluid Dynamic Theory of Two-Phase Flow, Collection de la Direction des Etudes et Recherches d'Electricite de France, Eyrolles, Paris.

Kieffer, S.W. (1981). 'Fluid dynamics of the May 18 blast at Mount St. Helens', U. S. Geol. Surv. Prof. Pap., 1250, 379-400.

Kieffer, S.W. (1982). 'Dynamics and thermodynamics of volcanic eruptions: Implications for the plumes on Io', in Satellites of Jupiter (Ed. D. Morrison), pp. 647-723, University of Arizona Press, Tucson.

Kieffer, S.W. (1984). 'Factors governing the structure of volcanic jets', in Explosive Volcanism: Inception, Evolution, and Hazards (Ed. F. R. Boyd), pp. 143-157, National Academy Press, Washington, D.C.

Kieffer, S.W., and Sturtevant, B. (1984). 'Laboratory studies of volcanic jets', J. Geophys. Res., 89, 8253-8268.

MacDonald, G.A. (1997). Volcanoes, Prentice-Hall, Englewood Cliffs, New Jersey.

Mercali, G., and Silvestri, D. (1891). 'Le eruzioni dell'isola di Vulcano, incominciate il 3 Agosta 1888 e terminate il 22 Marzo 1890: Relazione s ientifica 1891', Ann. Uff. Centr. Meterol. Geodent., 10(4), 135-148.

Shapiro, A.H. (1953). The Dynamics and Thermodynamics of Compressible Fluid Flow, Wiley, New York.

Smith, R.L. (1979). 'Ash flow magmatism', Geol. Soc. Amer. Spec. Pap., 180, 5-27.

Sparks, R.S.J., Wilson, L., and Hulme, G. (1978). 'Theoretical modeling of the generation, movement, and emplacement of pyroclastic flows by column collapse', J. Geophys. Res., 83, 1727-1739.

Travis, J.R., Harlow, F.H., and Amsden, A.A. (1975). 'Numerical calculation of two-phase flows', Los Alamos National Laboratory Report, LA-5942-MS, Los Alamos, New Mexico.

Ulam, S. (1980). 'Von Neumann: The interaction of mathematics and computing', in A History of Computing in the Twentieth Century (Eds. N. Metropolis, J. Howlett, and G.-C. Rota), pp. 93-99, Academic, New York.

Valentine, G.A., and Wohletz, K.H. (1989). 'Numerical models of plinian eruption columns and pyroclastic flows', J. Geophys. Res., 94, 1867-1887.

Valentine, G.A., and Wohletz, K.H. (in press). 'Environmental hazards of pyroclastic flows determined by numerical models', Geol.

Von Neumann, J., and Richtmyer, R.D. (1949). 'A method for the numerical calculation of hydrodynamic shocks', J. Appl. Phys., 21, 232-238.

Walker, G.P.L. (1973). 'Explosive eruptions--a new classification scheme', Geol. Rundsch., 62, 431-446.

Walker, G.P.L. (1981). 'Plinian eruptions and their products', Bull. Volcanol., 44, 223-240.

Wilson, L. (1980). 'Relationships between pressure, volatile content and ejecta velocity in three types of volcanic explosions', J. Volcanol. Geotherm. Res., 8, 297-313.

Wilson, L., Sparks, R.S.J., and Walker, G.P.L. (1980). 'Explosive volcanic eruptions, IV, The control of magma properties and conduit geometry on eruption column behavior', Geophys. J. Roy. Astron. Soc., 63, 117-148.

Wohletz, K.H., McGetchin, T.R., Sandford II, M.T., and Jones, E.M. (1984). 'Hydrodynamic Aspects of Caldera-Forming Eruptions: Numerical Models', J. Geophys. Res., 89, 8269-8285.

Woods, A.W. (1988). 'The fluid dynamics and thermodynamics of eruption columns', Bull. Volcanol., 50, 169-193.

Wright, J.K. (1967). Shock Tubes, Methuen, London.

FIGURE CAPTIONS

1. Plot of shock strength versus magma chamber overpressure.

2. Plot of velocities and temperature for analytical solution of shock-tube physics of the Bandelier Tuff eruption.

3. Distance-time plot for computer simulation of the blast that is thought to have initiated eruption of the Bandelier Tuff. The plot is analogous to an ideal one for a shock tube with propagation of a shock wave into the atmosphere while a rarefaction wave propagates down and reflects within the magma chamber and conduit. The contact surface marks the front of tephra and steam accelerated out of the vent. Both vertical and horizontal components are shown for these waves.

4. Schematic representation and marker particle plots at 13 seconds of simulated blast eruption time, showing the shock wave, ash contact, and rarefaction wave in the vent.

5. Developmental stages of a blast eruption followed by Plinian column collapse. The blast wave consists of a leading bow shock and trailing surges of tephra in which Mach disc shocks form in response to wide, nearly

hemispherically flaring of the overpressured jet as it expands into the atmosphere.

6. Plot of the collapse criterion for eruption columns in forming fountains. This plot is for a single tephra particle size and shows the control by Tg_m, Ri_m, and K_p, as defined by exit conditions. Exit conditions, plotting above the surface, form high-standing Plinian columns, while those plotting below the surface produce collapsing columns or fountains that lead to pyroclastic flow phenomena.

7. Numerical eruption simulation of a Plinian column. Contour plots of log θ_s with u_s, p, ρ_g, and T_s are shown for three times after initiation of discharge (10, 80, and 110 s). The innermost log θ_s contour corresponds to a solid volume fraction of 10^{-1}, and each contour outward represents an order of magnitude decrease in that value. Maximum flow speeds of about 400 m/s are attained in the basal 2 km of the column. The exit pressure of this eruption is 0.69 MPa, and the initial atmospheric pressure signal is shown in the pressure and gas-density plots at t = 10 s as a perturbation in the ambient values. T_s contours are drawn at 100 K intervals, starting at 1200 K at the vent, so that the outermost contour corresponds to 400 K. Note that as with all calculations, the atmosphere is initially density stratified and isothermal at 300 K.

8. Numerical eruption simulation of collapsing column or fountain. Contour plots are similar to those in Figure 7 and are shown for simulated eruption times of 10, 30, and 140 s. The exit pressure is atmospheric and maximum speeds are about 300 m/s at the exit plane. Note the atmospheric pressure signal at t = 10 s is better resolved than that shown in Figure 7, because the lower pressure of this eruption allowed drawing of closer pressure contours. High pressure cells are located at the elevation of collapse and where the collapsing flow impinges upon the ground. The contour plot of ρ_g at t = 140 s shows how hot, relatively low density gas is dragged beneath

the relatively high-density atmosphere, producing an unstable situation where the hot gas tends to rise out of the basal flow. This situation in turn leads to development of an ash cloud that buoyantly rises above the basal pyroclastic flow.

9. Simulated properties of a pyroclastic flow as functions of distance from the vent center: (a) horizontal velocity; (b) horizontal component of dynamic pressure; (c) temperature; and (d) particle volume fraction. Each of these parameters is shown for three times after the initiation of discharge (t = 109, 131, and 145 s), the earliest of which coincides with the initiation of the pyroclastic flow. For this eruption the flow conditions at the vent (200 m radius) are: velocity of 300 m/s, 0.2 mm particle diameter, 0.1 MPa (atmospheric) gas pressure, and a mass discharge of 9.0×10^8 kg/s.

10. Sketch of the flow field for multiphase flow in a lithospheric crack, which evolves into a flaring volcanic conduit.

Table 1. Notation.

c_0	sound speed of compressed gas
$\vec{g}$	gravitational acceleration
I_g	gas specific energy
I_s	solid specific energy
J	mass exchange rate
K_g	momentum exchange, particles to gas
K_s	momentum exchange, gas to particles
K_p	ratio of exit pressure to atmospheric pressure
M	Mach number
p	pressure
p_0	pressure of compressed gas
R_g	heat exchange, particles to gas
R_s	heat exchange, gas to particles
S_e	energy source of mass exchange and phase change
T_0	temperature of compressed gas
Tg_m	Thermogravitational parameter
t	time
Ri_m	Richardson number
r	spatial coordinate in radial direction
$\vec{u}_g$	gas velocity vector
$\vec{u}_s$	solid velocity vector
v	velocity
x	linear spatial coordinate
y	shock strength
z	spatial coordinate in vertical direction

Table 1. (Continued)

γ	gas isentropic exponent
ρ_g	gas microscopic density
ρ_s	solid microscopic density
ρ_0	density of compressed gas
μ	limit of isentropic expansion
θ_g	gas volume fraction
θ_s	solids volume fraction
τ	stress tensor
ν_e	eddy viscosity

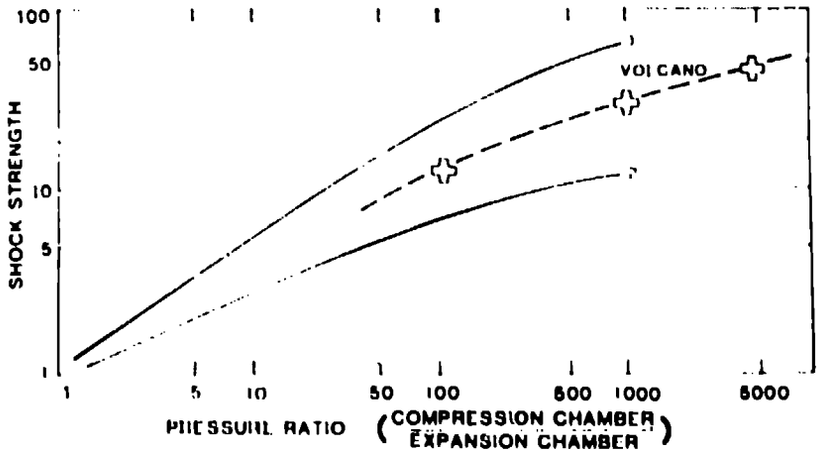
100
50
10
5
1
SHOCK STRENGTH
VOLCANO
1
5
10
50
100
500
1000
5000
PRESSURE RATIO (COMPRESSION CHAMBER / EXPANSION CHAMBER)

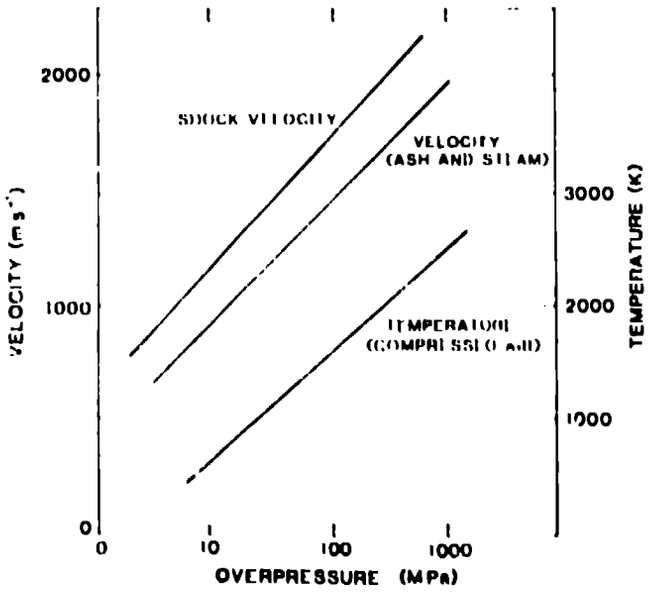
2000
1000
0
0
10
100
1000
OVERPRESSURE (MPa)
VELOCITY (m s⁻¹)
TEMPERATURE (K)
3000
2000
1000
SHOCK VELOCITY
VELOCITY
(ASH AND STEAM)
TEMPERATURE
(COMPRESSED AIR)

Fig 2.

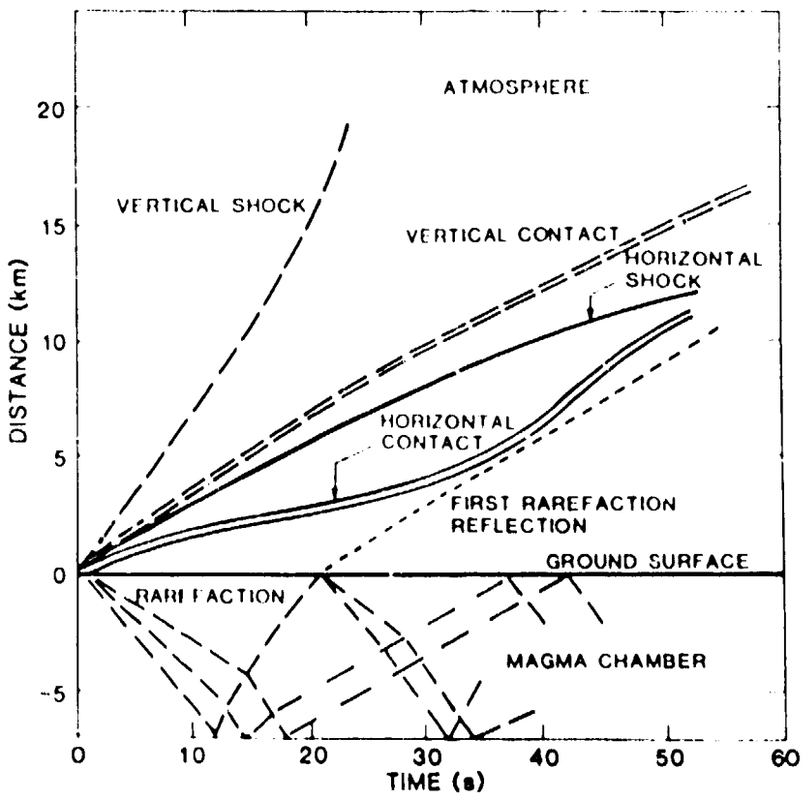
ATMOSPHERE
VERTICAL SHOCK
VERTICAL CONTACT
HORIZONTAL SHOCK
HORIZONTAL CONTACT
FIRST RAREFACTION REFLECTION
GROUND SURFACE
RAREFACTION
MAGMA CHAMBER
DISTANCE (km)
TIME (s)
20
15
10
5
0
-5
0
10
20
30
40
50
60

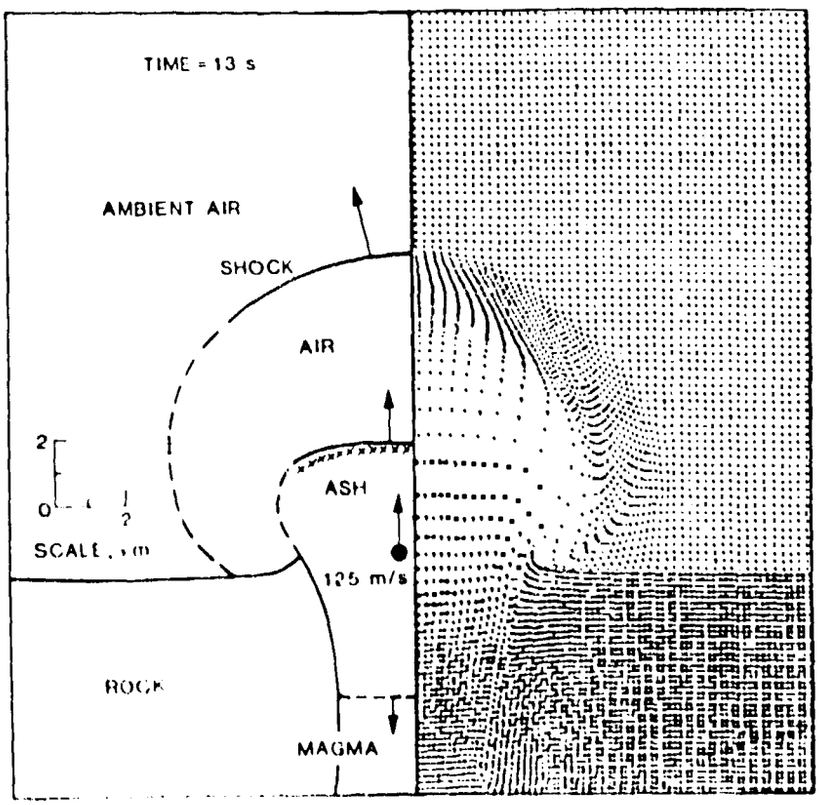
TIME = 13 s
AMBIENT AIR
SHOCK
AIR
ASH
125 m/s
ROCK
MAGMA
2
0
SCALE, m

Fig 4

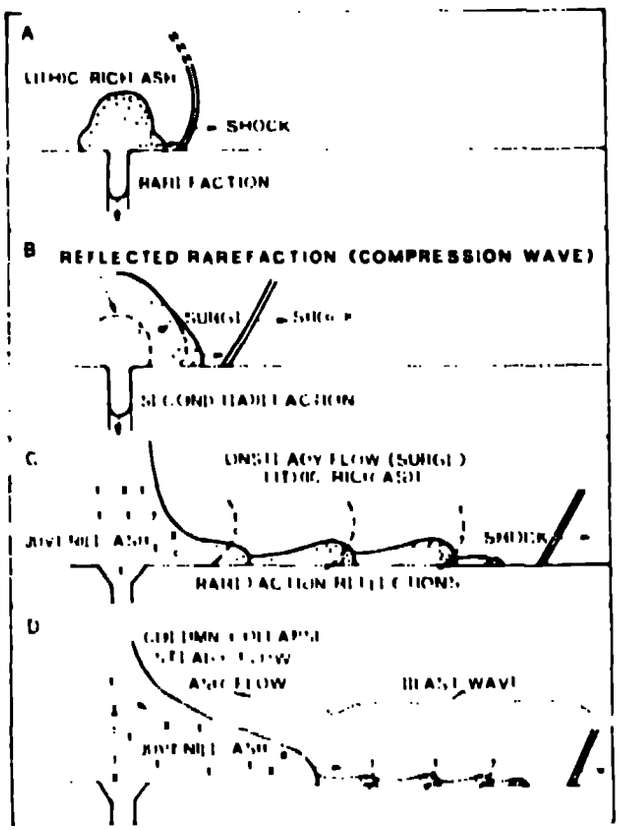
A
LITHIC RICH ASH
SHOCK
RAREFACTION
B
REFLECTED RAREFACTION (COMPRESSION WAVE)
SURGE
SHOCK
SECOND RAREFACTION
C
ONSET AGV FLOW (SURGE)
LITHIC RICH ASH
JUVENILE ASH
SHOCK
RAREFACTION REFLECTIONS
D
COLUMN COLLAPSE
PYROCLASTIC FLOW
ASH FLOW
BLAST WAVE
JUVENILE ASH

Fig 5

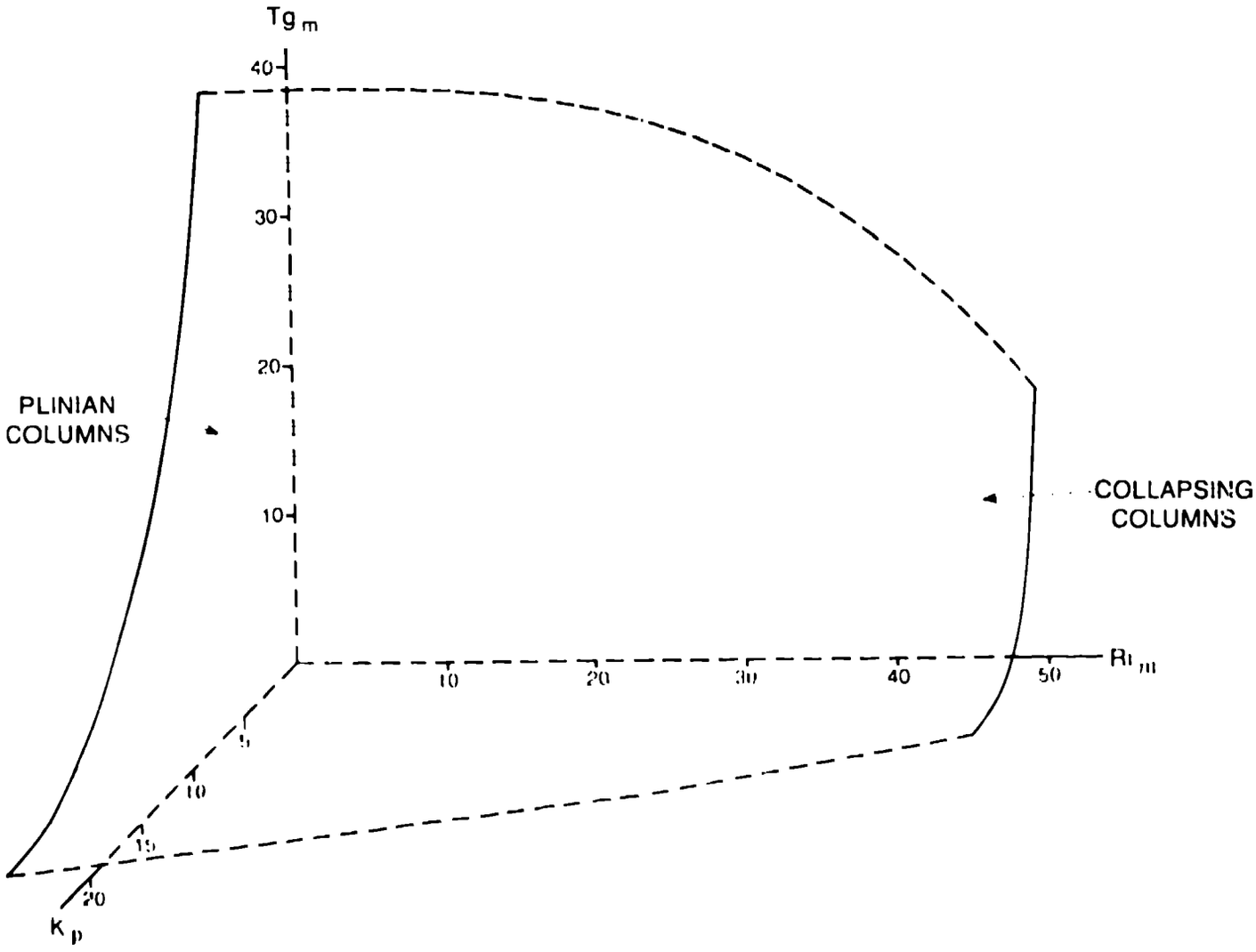
Tg m
40
30
20
10
PLINIAN
COLUMNS
COLLAPSING
COLUMNS
10
20
30
40
50
Ri m
5
10
15
20
K p

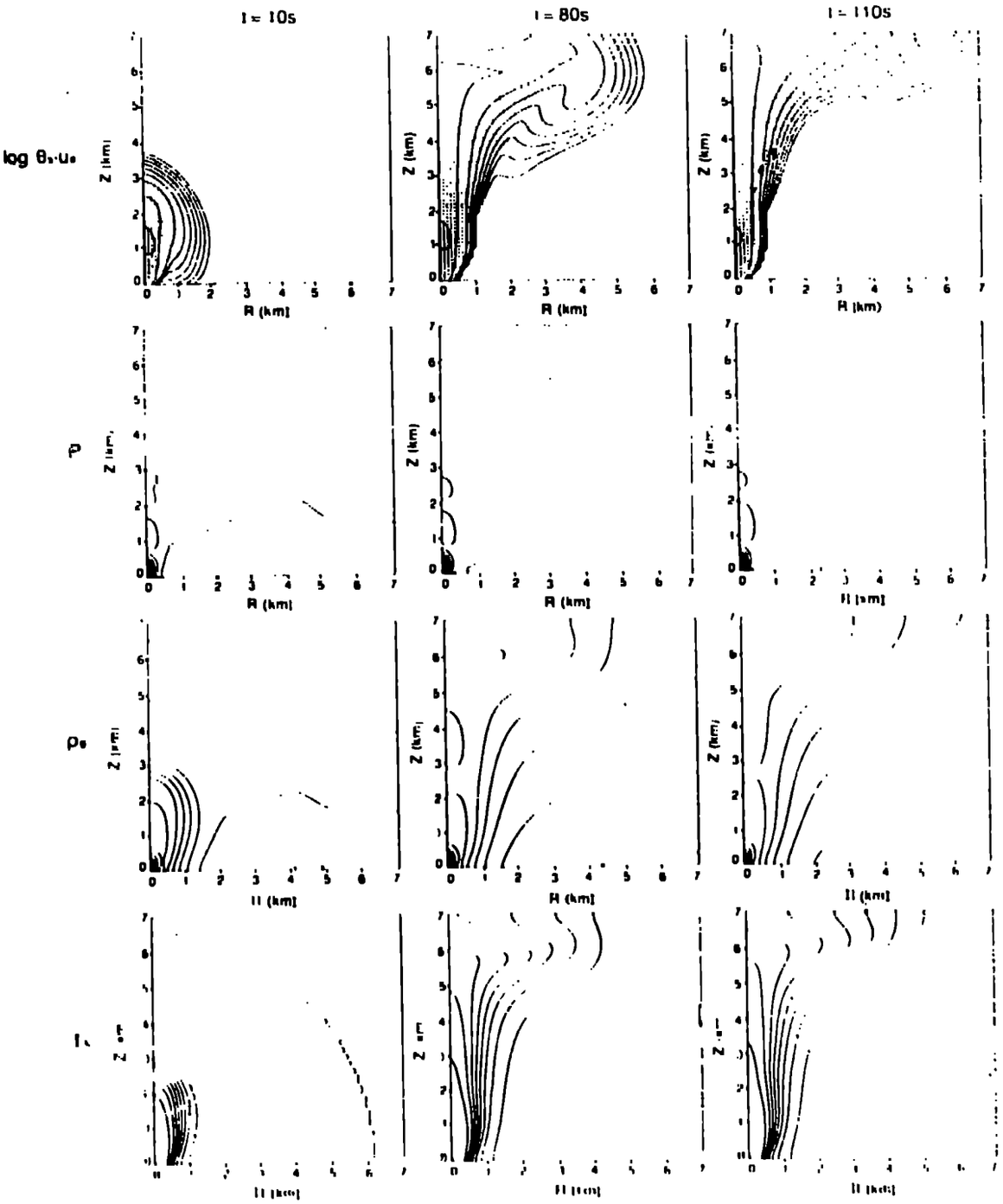
t = 10s
t = 80s
t = 110s
log θv-ue
Z (km)
R (km)

TOP

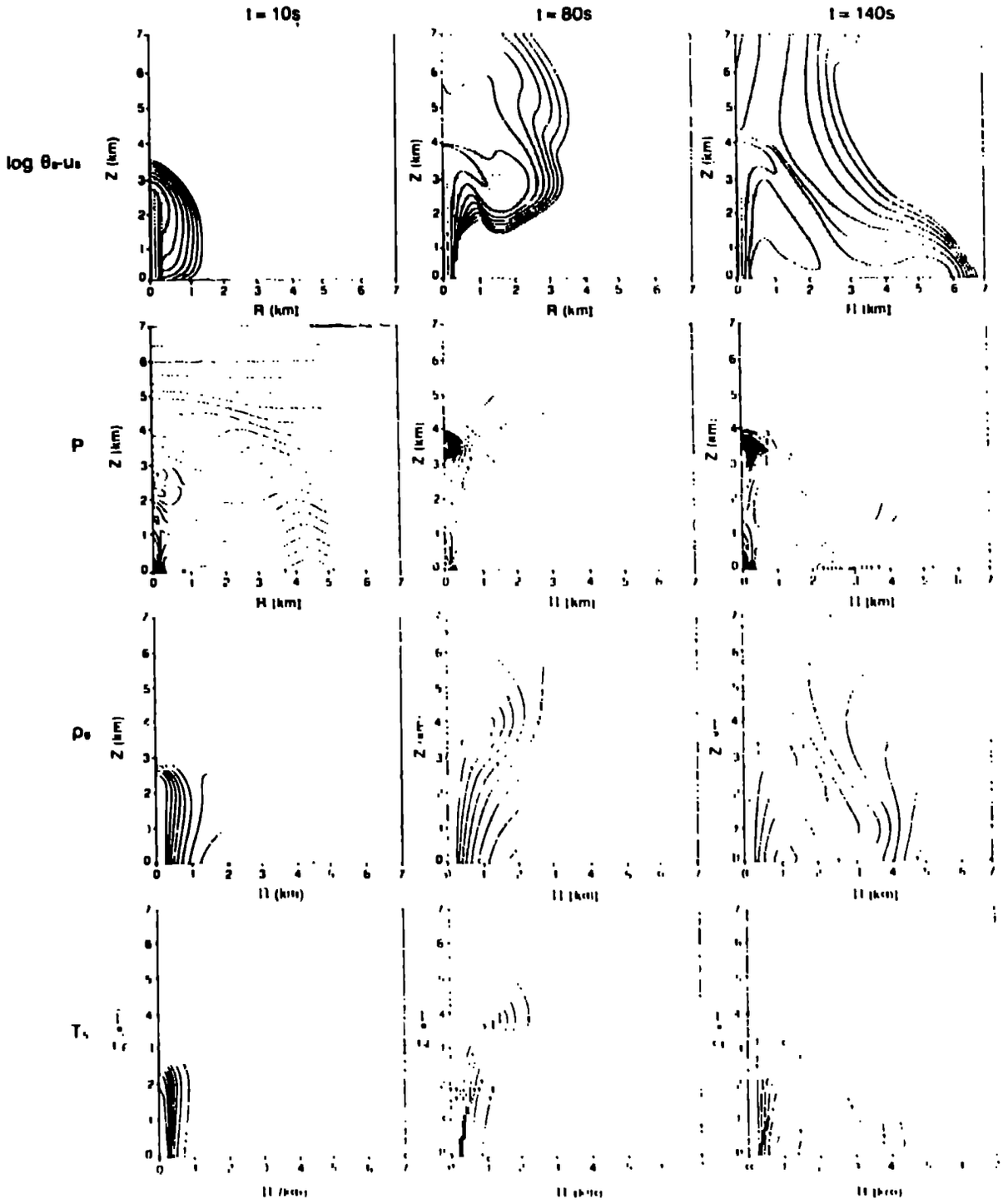

Fig 3

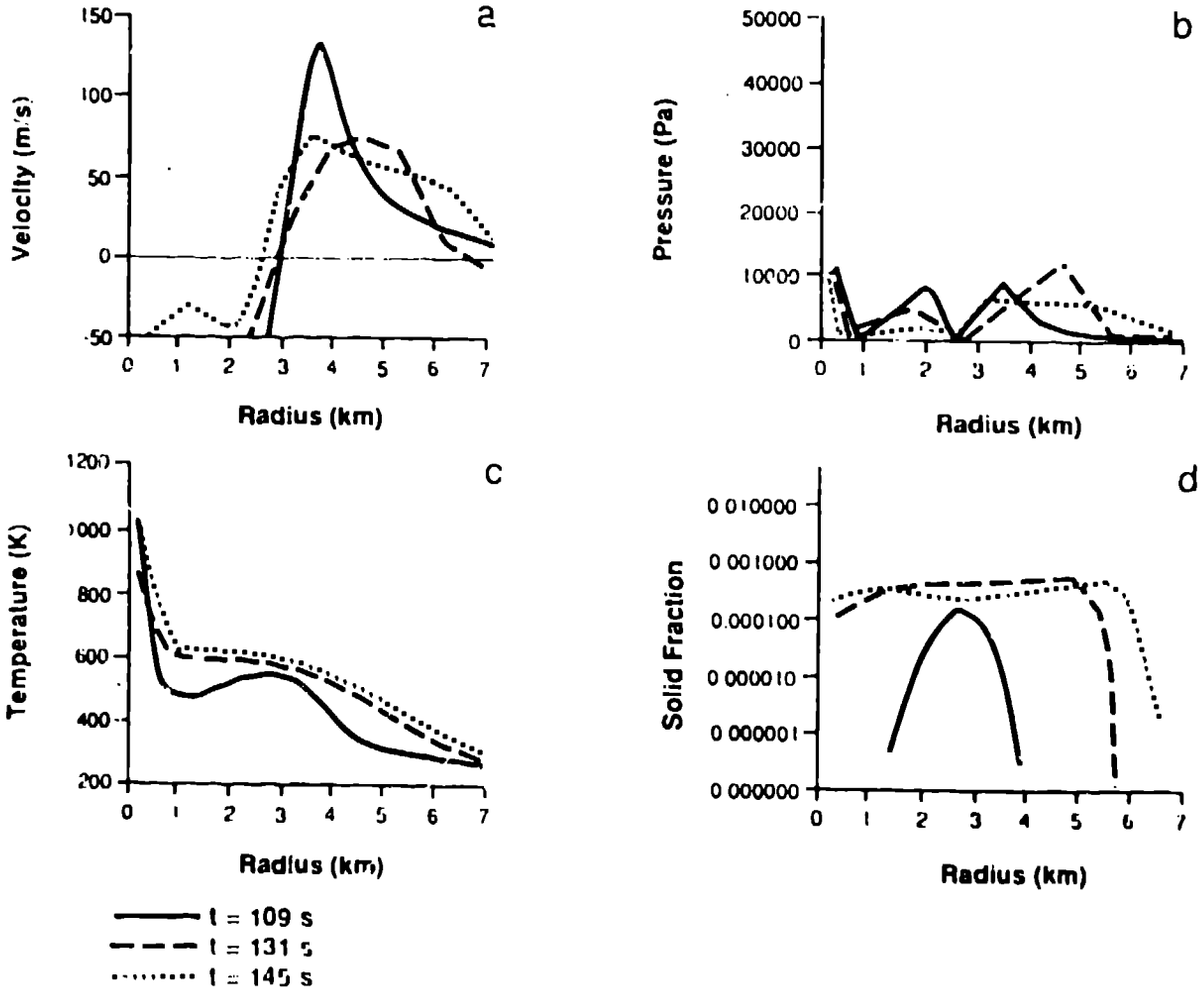
a
Velocity (m/s)
150
100
50
0
-50
0 1 2 3 4 5 6 7
Radius (km)
b
Pressure (Pa)
50000
40000
30000
20000
10000
0
0 1 2 3 4 5 6 7
Radius (km)
c
Temperature (K)
1200
1000
800
600
400
200
0 1 2 3 4 5 6 7
Radius (km)
d
Solid Fraction
0.010000
0.001000
0.000100
0.000010
0.000001
0.000000
0 1 2 3 4 5 6 7
Radius (km)
t = 109 s
t = 131 s
t = 145 s

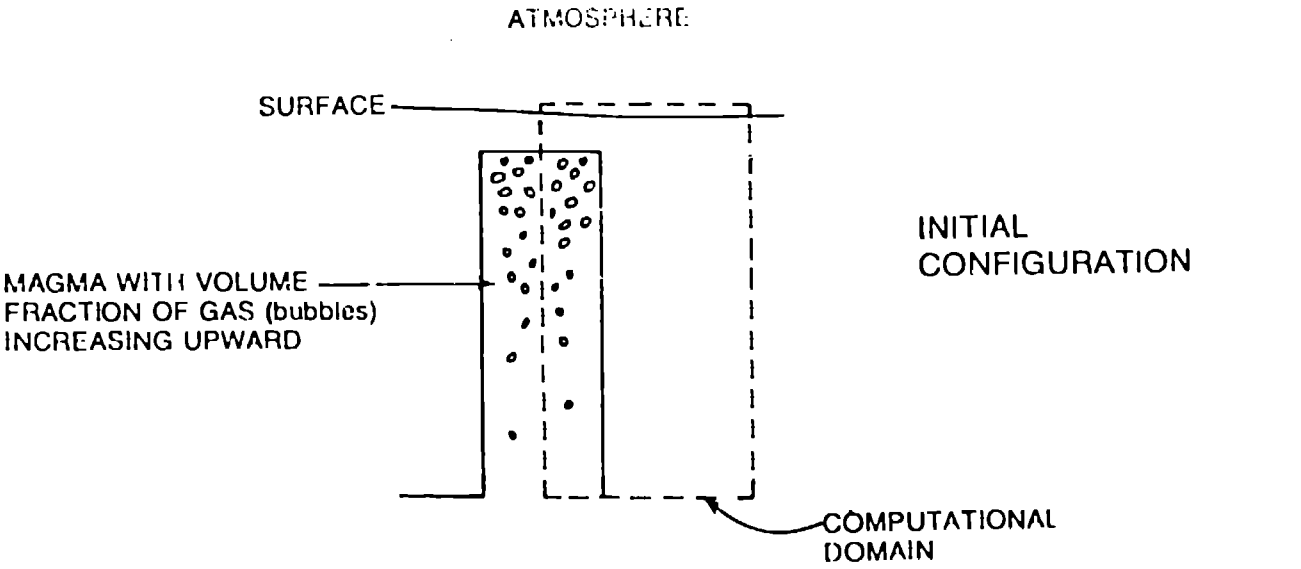
ATMOSPHERE
SURFACE
MAGMA WITH VOLUME FRACTION OF GAS (bubbles) INCREASING UPWARD
INITIAL CONFIGURATION
COMPUTATIONAL DOMAIN

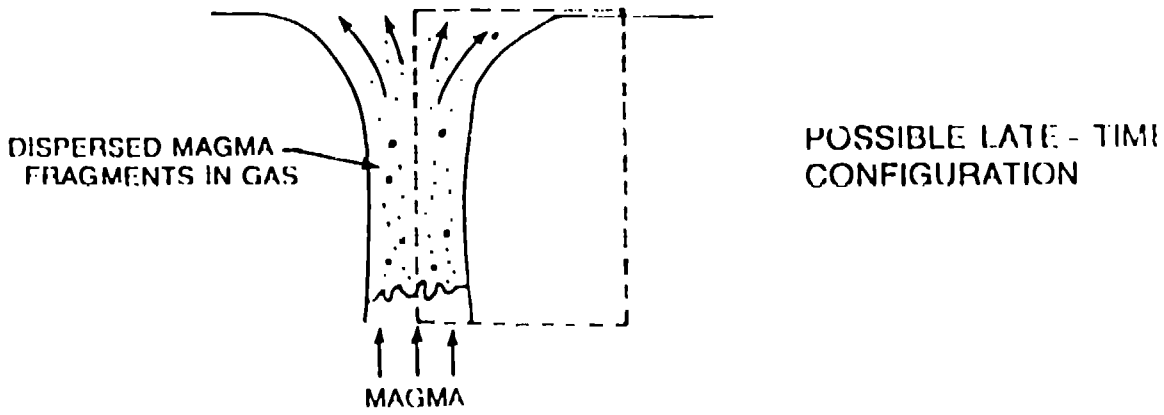
DISPERSED MAGMA FRAGMENTS IN GAS
MAGMA
POSSIBLE LATE - TIME CONFIGURATION